HUMAN ERYTHROCYTE ELECTROFUSION KINETICS MONITORED BY AQUEOUS CONTENTS MIXING

D. A. STENGER AND S. W. HUI
Electron Optics Laboratory, Roswell Park Memorial Institute, Buffalo, New York 14263

ABSTRACT The kinetics of electrically induced fusion of human erythrocyte ghosts were monitored by the Tb/DPA and ANTS/DPX fluorescence fusion assays. Ghosts were aligned by dielectrophoresis using a 3-MHz 350-V/cm alternating field and were fused by single 15- or 50-μs electric field pulses of amplitude 2.5–5.0 kV/cm. Fusion was detected immediately after the pulse. The peak fluorescence change due to fusion was always obtained within 7 s of pulse application, and was highest for a 5.0-kV/cm 15-μs pulse. Probe leakage was measured separately and became apparent only 2–3 s after the initiation of fusion. Increasing pulse amplitudes produced higher fusion yields but produced more leakage from the fusion products. 50-μs pulses produced less fusion, resulting from a disruption of the dielectrophoretic alignment by fluid turbulence immediately after pulse application. Probe leakage was observed only when pulse application was preceded by dielectrophoresis, suggesting that close membrane positioning allows for additional membrane destabilization caused by the high field pulse. The fluorescence kinetics are interpreted using a simplified model depicting three major types of events: (*a*) fusion without observable leakage, (*b*) fusion followed by probe leakage, and (*c*) contact-related leakage from ghosts which do not undergo contents mixing.

INTRODUCTION

Human erythrocytes and erythrocyte ghosts have frequently been used to characterize the electropermeation and electrofusion of mammalian cells (Zimmermann, 1982; Sowers, 1984). It is generally acknowledged that one or more high-voltage pulses are a prerequisite for fusion. However, the overall type and extent of membrane destabilization necessary for electrofusion is not well characterized (Sowers and Kapoor, 1987).

Recently, an ultrastructural model of erythrocyte electrofusion was reported (Stenger and Hui, 1986). It was proposed that an aqueous boundary (15–25 nm) separates adjacent erythrocytes aligned by dielectrophoresis. Fusion might be initiated in highly unstable regions, evidenced by membrane projections (100 nm across) observed to be predominantly free of intramembranous particles. Contact between apposed membranes appeared to be established after local disruption of the aqueous boundary and a temporary adhesion between the cells lasting several seconds after pulse application. Although a sequence of morphological changes may be reconstructed, complementary assays for monitoring fusion and leakage changes in a population of cells are also needed.

In this study, we use fluorescence fusion assays (Duzgunes and Bentz, 1986) to obtain kinetic data of the aqueous contents mixing and leakage for a population of erythrocyte ghosts undergoing electrofusion. It is undertaken to provide a quantitative means of comparing the kinetic events with proposed electrofusion models.

METHODS

Ghosts were prepared from fresh human erythrocytes by the method of Steck and Kant (1974) using 5 mM Na phosphate (pH 8) as the lysis buffer. The erythrocytes were washed three times in this buffer. The unsealed ghosts were held on ice until ready for use. Terbium (Tb)[1] and dipicolonic acid (DPA) were encapsulated into the ghosts as previously described (Hoekstra et al., 1985). 1.0 ml of packed, unsealed ghosts was resuspended in 10 ml of ice cold buffer solution (10 mM Hepes, pH 7.2) containing either Tb (7.5 mM) and citrate (75 mM) or DPA (75 mM) and NaCl (50 mM) and maintained at 0°C for 20 min. The ghosts were resealed by incubating the mixtures at 37°C for 45 min in the presence of 1 mM Mg. Nonencapsulated material was removed by washing once in buffer (145 mM NaCl, 10 mM Hepes at pH 7.2, with 1 mM EDTA) and twice again using the same without EDTA. Alternatively, ghosts were loaded in the same manner with 10 mM Hepes, pH 7.2, containing either 1-aminonaphthalene-3,6,8-trisulfonic acid (ANTS) (25 mM) and NaCl (110 mM) or *N,N'-p*-xylyenebis-(pyridinium bromide) (DPX) (90 mM) and NaCl (15 mM). It was shown (Hoekstra et al., 1985) that citrate prevents binding to Tb to the interior ghost membrane, and that passive leakage of the fluorophores from the ghosts was negligible in the experimental time frame. We observed that these criteria were also satisfied when using ANTS and DPX.

For each Tb/DPA fusion experiment, 1.5 μl each of packed Tb and DPA ghosts (18–20 μg protein) were resuspended in 200 μl of fusion medium containing 280 mM sucrose and 0.2 mM EDTA at pH 7.2. Fusion was measured by the development of the Tb:DPA complex

[1]Abbreviations used in this paper include: ANTS, 1-aminonaphthalene-3,6,8-trisulfonic acid; DPA, dipicolonic acid; DPX, *N, N'-p*-xylylenebis-pyridinium bromide; Tb, terbium.

fluorescence during contents mixing (Wilschut et al., 1980). The Tb/DPA fluorescence scale was calibrated to 100% using 3.0 μl of packed ghosts (containing 3.75 mM Tb, 37.5 mM citrate, 37.5 mM DPA, 25 mM NaCl, and 10 mM Hepes, pH 7.2) suspended in 200 μl of the fusion medium. The same type mixture was used for leakage experiments, measured as quenching of Tb:DPA fluorescence by the external EDTA. Greater than 95% of the Tb fluorescence was quenched by EDTA when the ghost contents were released into the fusion medium using Triton X-100. The same ghost concentrations and medium (less EDTA) were used for calibration, fusion, and leakage experiments when using ANTS and DPX. Calibration and intensity change measurements were analogously performed in accordance with the ANTS/DPX assay (Ellens et al., 1985). Fusion was detected as ANTS underwent collisional quenching by DPX.

Because of the high optical density of the sample, fluorescence was measured from the front surface of a fusion chamber made from a modified spectrophotometer cuvette (Type 19, NSG Precision Cells Inc., Hicksville, NY) shown in Fig. 1. The same modified cuvette was used to perform visual observations of dielectrophoresis and fusion in separate experiments. The fusion sequence was observed using a phase microscope (Olympus BH-2) and stored using a video recorder (Panasonic AG-6050). For fluorescence measurements, the sample material was enclosed in the fusion chamber, and the cuvette was placed in a holder and positioned with the front face at 45° to the excitation beam in a spectrofluorometer (Aminco-Bowman). Scattered and reflected light was removed by 7-54 bandpass and 3-72 cutoff filters (Corning Glass Works, Corning, NY) in the excitation and emission beams, respectively. A nonreflective metallic shield with a single slit (not shown) confined the light path to the chamber but allowed for the exposure of all chamber contents. The Tb/DPA was excited at 275 nm and fluorescence emission was monitored at 490 nm. ANTS was excited at 370 nm and fluorescence was measured at 515 nm.

The application of alternating and pulsed electric fields across the fusion chamber was controlled by an externally activated vacuum relay (Fig. 2). For each experiment, a 3-MHz 350-V/cm alternating field was applied for 15 s before and 40 s after the application of a single pulse of variable amplitude and width. The changes in fluorescence during fusion were measured by a photon counter having a sampling period of 30 ms. The signal noise level was ~3% of the full scale reading. All experiments were initiated at room temperature (20°C). The maximum temperature increase possible during the experiment was simulated using a mixture of 1.5 μl each of the Tb and DPA solutions in 200 μl of fusion medium. This mixture was sealed in the fusion chamber and exposed to the experimental electric field applications. The temperature increase was measured directly with a thin wire thermocouple junction positioned in the medium between the electrodes. The temperature increased by 3–4°C after 60 s of alternating field application. None of the pulses used in the experiments individually caused an observable increase.

Tb-containing ghosts showed reduced dielectrophoresis when stored as a concentrated pellet for >90 min. This effect was fully reversed by rewashing them once with buffer (145 mM NaCl, 10 mM Hepes, pH 7.2, and 0.2 mM EDTA). Control experiments confirmed that the intrinsic properties of the encapsulated fluorophores were not observably affected by the applied electric fields or the resulting temperature increase and that the fluorescence calibration scale was not dependent on the relative orientation or aggregation of the cells.

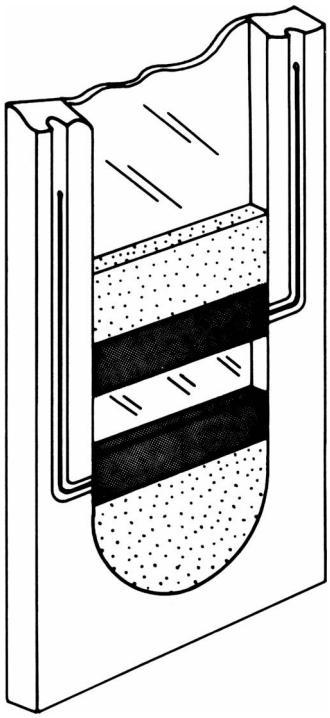

FIGURE 1 Fluorometric fusion chamber. Two flat stainless steel electrodes (*dark bars*) were mounted horizontally on the rear window of the demountable cell at a separation of 600 μm and machined to be flush with the back surface of front window when the cell was closed. The entire sample could then be uniformly subjected to the applied electric fields. The surrounding enclosed volume of the rear window was permanently filled with epoxy resin (*dotted pattern*). The application of high vacuum grease to the front surfaces of the electrodes and window contact sites before each experiment promoted a tight sealing of the chamber once the cell was closed. The chamber contents were easily viewed by phase microscopy if an ordinary glass coverslip was substituted for the front window of the cell.

RESULTS AND DISCUSSION

Initially, the suspended ghosts formed rigid pearl chains in the chamber regardless of the composition of their contents (Fig. 3 *A*). Within 40 s of application of a single 15 μs pulse of amplitude 2.5–5.0 kV/cm to the ghost suspension, a variable fraction of the cells visibly fused and/or began to gradually cluster on the electrode surfaces (Fig. 3 *b*). Because many cells became rearranged after pulse application, an accurate quantitation of the fusion yield could not be determined by microscopy. If the ghosts were prepared from erythrocytes treated with neuraminidase (50 μg/ml, 37°C, 30 min), the same type of aggregation led to the formation of large spherical fusion products (diameter

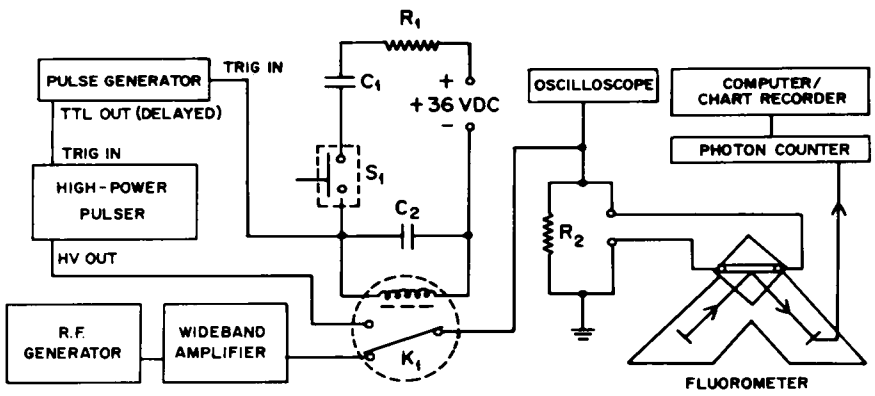

FIGURE 2 Experimental setup. An externally activated vacuum relay, K_1, is used to switch between alternating and pulse circuits. When the manual switch (S_1) is depressed, K_1 is switched from the alternating current to the pulse circuit for 100 ms, and a triggering signal activates a high-power pulse generator (Velonex, model 345). The negative, rectangular, high-power pulse is delayed by 50 ms to position it near the center of the 100-ms alternating-field off-period.

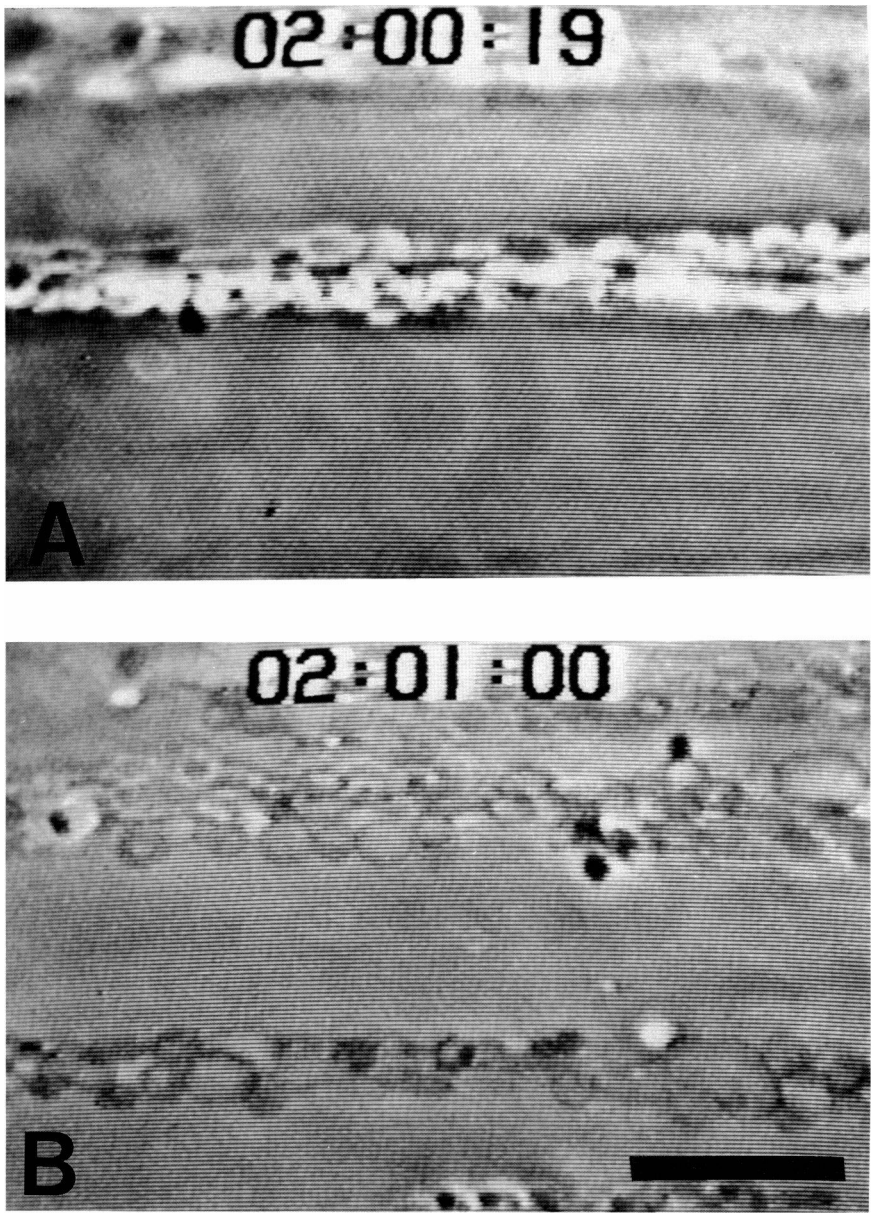

FIGURE 3 Phase micrographs of dielectrophoresis and fusion inside the fluorometric fusion chamber. (*A*) A 1:1 mixture of Tb- and DPA-containing ghosts are aligned in a 350-V/cm, 3-MHz alternating field. (*B*) At 40 s after a 15-μs, 5.0-kV/cm pulse. Bar, 25 μm.

>250 μm) within 5 min (not shown). Because preliminary results indicated that large fluorescence changes could be detected without neuraminidase treatment, we focused on the fusion of untreated ghosts.

Fig. 4 illustrates the relative Tb fluorescence changes after application of single 15-μs pulses of increasing amplitude to dielectrophoretically aligned ghosts at time = 0. The fusion curves (*solid lines*) indicating the percent of maximal Tb and DPA mixing reflected that fusion occurred immediately after pulse application, and peaked at a later time. The fluorescence level usually dropped, due to leakage of Tb:DPA from fusion products (and to a lesser extent by the influx of EDTA). Pronounced leakage was detected from the fusion products as the pulse amplitude was doubled from 2.5 to 5.0 kV/cm. The total leakage, which was measured in separate experiments as the quenching of coencapsulated Tb and DPA (Fig. 4., dashed lines), became apparent only after a 2–3 s lag period after pulse application, and increased by only ~50% over the same range of pulse amplitudes. Fusion and probe leakage were not observed if the cells were not first aligned by the alternating field or if pulse amplitudes of <2.0 kV/cm were used.

To further validate the results obtained using Tb and DPA, we also utilized the ANTS/DPX assay. Phase microscopy observations (not shown) revealed that although ANTS- and DPX-containing ghosts aligned equally well in the alternating field, many dissociated within several seconds after pulse application, apparently due to decreased dielectrophoretic force (as distinguished from turbulence-induced disruption). This effect is understandable, considering the strong dependence of the dielectrophoretic force on the ionic composition of the suspending medium (Pohl, 1978), which is altered when the ghosts

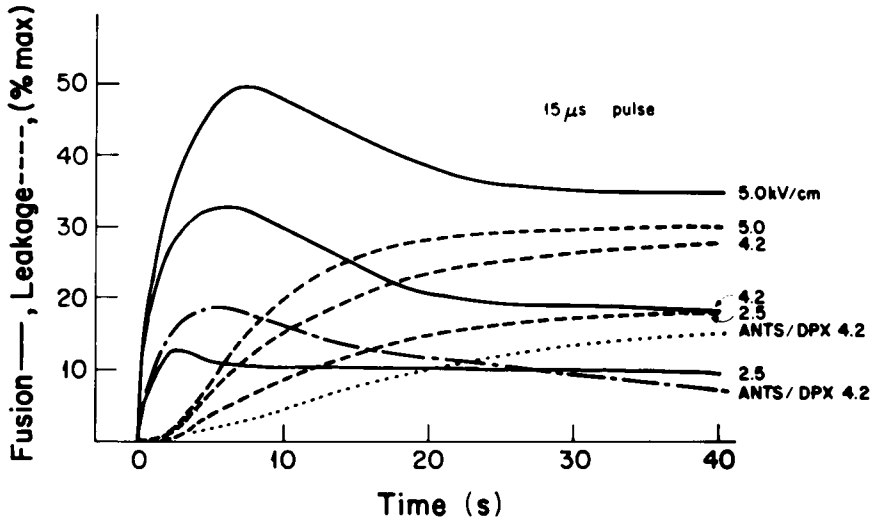

FIGURE 4 Fusion and leakage kinetics of dielectrophoretically aligned erythrocyte ghosts caused by single 15-μs pulses of increasing amplitude applied at time = 0. Fusion of Tb- and DPA-containing ghosts (*solid lines*) was measured as the increased fluorescence produced by contents mixing. Leakage (*dashed lines*) was determined in separate experiments as the decreased fluorescence caused by quenching of Tb:DPA fluorescence by external EDTA in the fusion medium. The fusion of ANTS- and DPX-containing ghosts (*solid/dotted line*) was measured as the percentage of maximal ANTS fluorescence quenched due to contents mixing. Leakage (*dotted line*) was measured in separate experiments as the relief of ANTS quenching from ghosts encapsulated with a 1:1 ratio of ANTS and DPX mixtures.

leak. It is known that some smaller ions, including Na, pass through the erythrocyte membrane during pulse application (Teissie and Tsong, 1980). It may be that the ionic leakage from the ANTS and DPX ghosts during pulse application causes a more pronounced reduction of dielectrophoretic force than that from Tb- and DPA-containing ghosts. From the phase microscopy observations, we would expect that corresponding changes in fusion fluorescence would also occur. Fig. 4 also shows the fluorescence changes caused by fusion of a 1:1 mixture of a dielectrophoretically aligned ANTS- and DPX-containing ghosts (*dashed and dotted line*) and leakage (*dotted line*) from the same amount of ghosts with coencapsulated ANTS and DPX after application of a 15 μs, 4.2 kV/cm pulse at time = 0. Although the percentages of the maximum fluorescence changes were different, the initial slopes and relative curve shapes were quite similar for the two types of ghost mixtures. Because the microscopy-observed fusion of the Tb- and DPA-containing ghosts more closely paralleled that observed of unloaded ghosts, they were used exclusively in subsequent experiments.

The effects of wider pulses were also examined. Phase microscopy (not shown) revealed that the pearl chain alignment was significantly disrupted within 1 s after application of a 50-μs pulse. The cause of this disruption was the fluid turbulence in the chamber. The corresponding changes in Tb fluorescence due to a 50-μs pulse of varying amplitude are shown in Fig. 5. The percentage of maximum fluorescence due to fusion (*solid lines*) was sharply reduced relative to that when using a 15-μs pulse of the same amplitude. The observed total leakage (*dashed lines*) was also correspondingly reduced, except in the case of a 5.0-kV/cm pulse. When a 100-μs pulse was used (results not shown), the effect was similar. Again neither fusion nor leakage was observed when using pulse amplitudes of <2.0 kV/cm, or when ghosts were not first aligned in an alternating field.

The corrected fusion fluorescence, I_t, may be derived

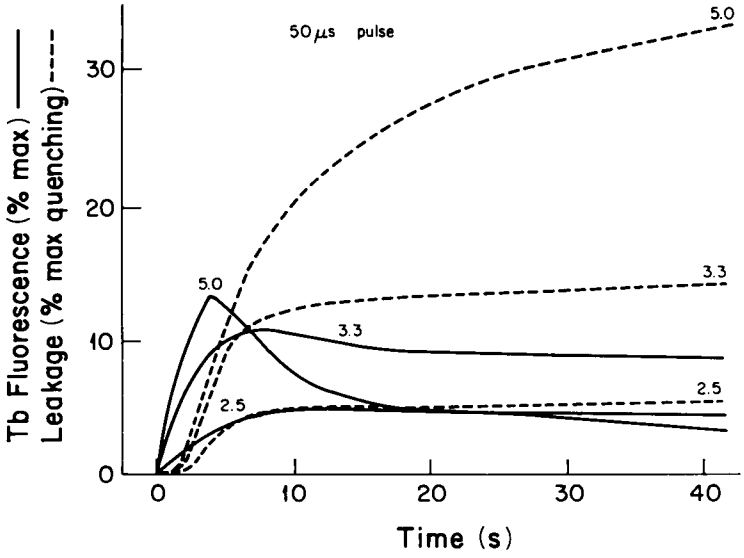

FIGURE 5 Fusion (*solid lines*) and leakage (*dashed lines*) for a 1:1 mixture of Tb- and DPA-containing ghosts after application of a 50-μs pulse of varying amplitude applied at time = 0.

from the observed percentage of maximum fluorescence I_{obs} and the percent of total leakage, L_t, (Duzgunes and Bentz, 1986) by

$$I_t = I_{obs} + \delta L_t.$$

δ represents the fraction of fused ghosts containing both Tb and DPA or both ANTS and DPX. We modeled the relative changes in fusion and leakage events as depicted in Fig. 6. *A* represents a fusion event (binary or higher order) accompanied by very minor leakage. This type of fusion produces the fast initial rise in fusion fluorescence preceding the onset of observable leakage. Fig. 6 *B* represents those fusion events which are followed by a relatively large loss of encapsulated contents. This type becomes apparent as the decrease of fusion fluorescence from the peak intensity. Fig. 6 *C* represents a contact-related leakage from ghosts which have not undergone contents-mixing. This event appears as the difference between the total measured leakage and that which is necessary to reduce the fusion fluorescence (via B type leakage), even if only binary fusions occur (i.e., $\delta = 0.5$).

Accordingly, a 15-μs 2.5-kV/cm pulse (Fig. 4) immediately produces stable A products and a subpopulation exhibiting type C leakage. 15-μs pulses of 4.2 and 5.0 kV/cm also produce exclusively A products for the first several seconds, but with an increased type B leakage. The B/C and A/C ratios increase with increasing pulse amplitude. The data for 15-μs pulses collectively suggests that (*a*) as the pulse amplitude is raised from 2.5 to 5.0 kV/cm, more ghosts fuse, but at the expense of increasing type B leakage, and (*b*) after the 2.5 kV/cm pulse, a subpopulation of ghosts are damaged enough to leak but not fuse. This subpopulation (type C) becomes less significant with higher amplitude pulses, as the total percentage of fused cells increases.

When 50-μs pulses are used (Fig. 5), the dielectrophoretic alignment is increasingly disrupted by higher voltage pulses. A small percent of stable A type products are apparently formed at 2.5 and 3.3 kV/cm, whereas at 5.0 kV/cm the relative amount of B type fusion products is again increased. In contrast to that observed after applying 15-μs pulses, the amount of leakage from unfused ghosts appears to be maximal for the 5.0-kV/cm pulse. This suggests that (*a*) increasing the pulse amplitude again increases fusion at the expense of membrane damage, and (*b*) although fusion may immediately occur in some cells, high-fusion yields are dependent on the maintenance of the pearl chain structures for at least several seconds after pulse application.

One significant observation is that there is no detectable fusion or leakage if the ghosts are not aligned and closely positioned by dielectrophoresis before pulse application. This is not in disagreement with the directly observed pulse-induced efflux of fluorescent molecules across the membranes of isolated ghosts (Sowers and Lieber, 1986), because significantly different probes and pulse parameters were used. Our results show only that any "pores" which may have been produced in the membranes of nonaligned, isolated ghosts by 15- or 50-μs pulses of 5.0 kV/cm or less are impermeable to fluorescence probes used. Short-lived (~100 ms), destabilized membrane areas were observed in the membranes of both aligned and isolated erythrocytes by electron microscopy (Stenger and Hui, 1986). If such areas are necessary for the electrofusion of ghosts, it is unlikely that they represent perforations which are permeable to the fluorescent probe molecules used in this study.

The observed contact-dependent leakage must result from additional types of membrane destabilization than that producing the transient dielectric breakdown in isolated ghosts. The increased damage to fused membranes with increasing pulse amplitudes may be of general interest, pertaining to the viability of hybrid cells. Most of the probe leakage from unfused ghosts (type C) begins 10–15 s after pulse application. This indicates an event that occurs later in time than fusion (type A) and the leakage from fusion products (type B). Sowers (1984) showed that a large percentage of ghosts may adhere and exchange lipid-soluble probes without contents mixing after pulse application. Similarly, we observed ultrastructural defects suggesting temporary intermembrane contact during the fusion of enzymatically treated erythrocytes (Stenger and Hui, 1986). Thus, the later-occurring membrane destabilization may be closely related to the physical separation of previously adhered membranes.

In summary, the kinetics of electrofusion may be monitored using well-established fluorescence fusion assays. However, proper care must be exercised in the interpretation of results obtained when varying the intracellular and extracellular ionic composition. Although the formation of aqueous electropores is frequently regarded as a prerequisite for fusion, both the Tb/DPA and ANTS/DPX assays suggest that there is not a direct correspondence between pulse-induced efflux of the fluorescent probes and the initiation of electrofusion.

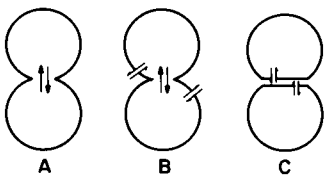

FIGURE 6 Simplified model of the three major events which may account for the observed fusion kinetics. (*A*) Fusion products that have lost an unobservable amount of fluorescent contents. (*B*) Fusion products that show considerable leakage. (*C*) Contact-related leakage from unfused ghosts.

The technical assistance of W. Beers is greatly appreciated.

This work was supported by National Institutes of Health grant GM 30969 awarded to S.W.H.

Received for publication 20 April 1987 and in final form 18 September 1987.

REFERENCES

Duzgunes, N., and J. Bentz. 1986. Spectroscopic Membrane Probes. L. M. Loew, editor. CRC Press, Boca Raton, FL.

Ellens, H., J. Bentz, and F. C. Szoka. 1985. H^+ and Ca^{++}-induced fusion and destabilization of liposomes. *Biochemistry.* 24:3099–3106.

Hoekstra, D., J. Wilschut, and G. Scherphof. 1985. Fusion of erythrocyte ghosts induced by calcium phosphate. *Eur. J. Biochem.* 146:131–140.

Pohl, H. A. 1978. Dielectrophoresis. Cambridge University Press, London.

Sowers, A. E. 1984. Characterization of electric field-mediated fusion in erythrocyte ghost membranes. *J. Cell Biol.* 99:1989–1996.

Sowers, A. E., and V. Kapoor. 1987. The electrofusion mechanism in erythrocyte ghosts. *In* Cell Fusion. A. E. Sowers, editor. Plenum Publishing Corp., New York. 397–408.

Sowers, A. E., and M. Lieber. 1986. Electropore diameters, lifetimes, numbers, and locations in individual erythrocyte ghosts. *FEBS (Fed. Eur. Biochem. Soc.) Lett.* 205:179–184.

Steck, T. L., and J. A. Kant. 1974. Preparation of impermeable ghosts and inside-out vesicles from human erythrocyte membranes. *Methods Enzymol.* 31:172–180.

Stenger, D. A., and S. W. Hui. 1986. The kinetics of ultrastructural changes during electrically-induced fusion of human erythrocytes. *J. Membr. Biol.* 93:43–53.

Teissie, J., and T. Y. Tsong. 1980. Evidence of voltage-induced channel opening in Na/K ATPase of human erythrocyte membrane. *J. Membr. Biol.* 55:133–140.

Wilschut, J., N. Duzgunes, R. Fraley, and D. Papahadjopoulos. 1980. Studies on the mechanism of membrane fusion: kinetics of calcium ion induced fusion of phosphatidylserine vesicles followed by a new assay for mixing of aqueous vesicle contents. *Biochemistry.* 19:6011–6021.

Zimmerman, U. 1982. Electric field mediated fusion and related electrical phenomena. *Biochim. Biophys. Acta.* 694:227–277.